Spatio-temporal dynamics in semiconductor microresonators with thermal effects

Giovanna Tissoni, Lorenzo Spinelli and Luigi A. Lugiato

INFM, Dipartimento di Scienze Chimiche, Fisiche e Matematiche, Università dell'Insubria, via Valleggio 11, 22100 Como, Italy

tissoni@mi.infn.it

Massimo Brambilla, Ida M. Perrini and Tommaso Maggipinto

INFM, Dipartimento di Fisica Interateneo, Università e Politecnico di Bari, via Orabona 4, 70126 Bari, Italy

Abstract: In this paper we study the dynamics of the intracavity field, carriers and lattice temperature in externally driven semiconductor microcavities. The combination/competition of the different time-scales of the dynamical variables together with diffraction and carrier/thermal diffusions are responsible for new dynamical behaviors. We report here the occurrence of a spatio-temporal instability of the Hopf type giving rise to Regenerative Oscillations and travelling patterns and cavity solitons.

OCIS codes: (190.4420) Nonlinear optics, transverse effects in; (190.4870) Optically induced thermo-optical effects; (160.6000) Semiconductors, including MQW

References and links

1. L. A. Lugiato, M. Brambilla and A. Gatti, "Optical Pattern Formation," in Advances in Atomic, Molecular and Optical Physics, Vol. **40**, edited by B. Bederson and H. Walther, Academic Press, 1998, pp. 229-306, and references quoted therein.
2. N. N. Rosanov and G. V. Khodova, "Autosolitons in bistable interferometers," Opt. Spectrosc. **65**, 449-450 (1988).
3. M. Tlidi, P. Mandel and R. Lefever, "Localized structures and localized patterns in optical bistability," Phys. Rev. Lett. **73**, 640-643 (1994).
4. W. J. Firth and A. J. Scroggie, "Optical bullet holes: robust controllable localized states of a nonlinear cavity," Phys. Rev. Lett. **76**, 1623-1626 (1996).
5. M. Brambilla, L. A. Lugiato and M. Stefani, "Interaction and control of optical localized structures," Europhys. Lett. **34**, 109-114 (1996).
6. M. Saffman, D. Montgomery and D. Z. Anderson, "Collapse of a transverse-mode continuum in a self-imaging photorefractively pumped ring resonator," Opt. Lett. **19**, 518-520 (1994).
7. V. B. Taranenko, K. Staliunas and C. O. Weiss, "Spatial soliton laser: localized structures in a laser with a saturable absorber in a self-imaging resonator," Phys. Rev. A **56**, 1582-1591 (1997).
8. B. Schaepers, M. Feldmann, T. Ackemannand, W. Lange, "Interaction of Localized Structures in an Optical Pattern-Forming System," Phys. Rev. Lett. **85**, 748-751 (2000).
9. S. Barland, J.R. Tredicce, M. Brambilla, L. A. Lugiato, S. Balle, M. Giudici, T. Maggipinto, L. Spinelli, G. Tissoni, T. Koedl, M. Miller and R. Jaeger, "Cavity solitons work as pixels in semiconductors," Nature, to appear. See also references quoted therein.
10. L. Spinelli, G. Tissoni, M. Brambilla, F. Prati and L. A. Lugiato, "Spatial solitons in semiconductor microcavities," Phys. Rev. A **58**, 2542-2559 (1998) and references quoted therein.
11. L. Spinelli, G. Tissoni, M. Tarenghi and M. Brambilla, "First principle theory for cavity solitons in semiconductor microresonators," Eur. Phys. J. D **15**, 257-266 (2001) and references quoted therein.
12. E. Abraham, "Modelling of regenerative pulsations in an InSb etalon," Opt. Comm. **61**, 282-286 (1987) and references quoted therein.
13. S. Barland, O. Piro, S. Balle, M. Giudici and J. Tredicce, "Thermo-optical pulsation in semiconductor lasers with injected signal: Relaxation oscillations, excitability, phase-locking and coherence resonance," preprint.

#1519 - $15.00 US Received August 01, 2002; Revised September 13, 2002

14. R. Kuszelewicz *et al.*, 2nd yearly report of the PIANOS Project (2000). I. Ganne, Ph. D. Thesis (2000).
15. L. Spinelli, G. Tissoni, L. A. Lugiato and M. Brambilla, "Thermal instabilites in semiconductor amplifiers," submitted to J. Mod. Opt., special issue for the Proceedings of the Physics of Quantum Electronics Conference (Snowbird USA January 6-10, 2002) edited by R. W. Boyd and M. O. Scully.
16. L. Spinelli, G. Tissoni, L. A. Lugiato and M. Brambilla, "Thermal effects and transverse structures in semiconductor microcavities with population inversion," Phys. Rev. A **66**, 023817 (2002).
17. A. J. Scroggie, J. M. McSloy and W. J. Firth, "Self-Propelled Cavity Solitons in Semiconductor Microcavities," submitted to Phys. Rev. E.
18. T. Rossler, R. A. Indik, G. K. Harkness, J. V. Moloney and C. Z. Ning, "Modeling the interplay of thermal effects and transverse mode behavior in native-oxide-confined vertical-cavity surface-emitting lasers," Phys. Rev. A **58**, 3279-3292 (1998).

1 Introduction

Transverse pattern formation in nonlinear optical systems [1] has raised a noteworthy attention in the last decade, both from a fundamental viewpoint and, more recently, for the potential applications to information technology. In the latter framework, especially interesting is the possibility of generating spatial structures that are localized in a portion of the transverse plane in such a way that they are individually addressable and independent of one another and of the boundary. Such structures, called Cavity Solitons (CS) have been theoretically predicted in nonlinear materials inside a cavity (see *e.g.* [2, 3, 4, 5]) and experimentally observed in macroscopic cavities (see *e.g.* [6, 7]) and in feedback systems (see *e.g.* [8]).

Most interesting from the practical viewpoint, for miniaturization purposes, is the case in which the active medium is a semiconductor: the standard configuration on which we will focus our attention is that of an optical cavity containing a semiconductor medium and driven by a stationary holding beam, which provides the energy to the system. Both the material sample and the holding beam have a large section.

This research has been carried out in the framework of the ESPRIT Long Term Project PIANOS (Processing of Information with Arrays of Nonlinear Optical Solitons), in close connection with experimental activity in progress at INLN (Nice), LPN (Marcoussis) and PTB (Braunschweig), on active and passive semiconductor microcavities. The aim of the project is to demonstrate the existence of CS in semiconductor microresonators, and the possibility of using them as binary units for all-optical information treatment. An especially clear experimental demonstration of CS in semiconductor devices has been recently obtained [9].

In recent papers [10] a number of phenomenological models have been proposed in order to describe the semiconductor material. On the other hand, a more accurate modelization of the semiconductor material, including a microscopic description of the optical nonlinearity has been performed in [11]. For such models existence and stability of CS have been theoretically predicted, for both the case with and without injection of carriers.

In this paper, we want to study the effect of the thermal dynamics on spatial structures in general and on CS in particular in semiconductor devices. Precisely, we focus our attention on semiconductor microresonators containing either a passive bulk GaAs or an active, *i.e.* with population inversion, Multi-Quantum-Well structure.

From the existing literature on fundamental thermal effects in semiconductor devices [12], it is well known that the combination/competition of the (slow) temperature nonlinearity and the (fast) carrier nonlinearity forces the system to peculiar behaviors. For example, in a recent work [13] an experimental observation of temporal oscillations in laser diodes is reported, and a theoretical interpretation of such a behavior is given in

#1519 - $15.00 US Received August 01, 2002; Revised September 13, 2002

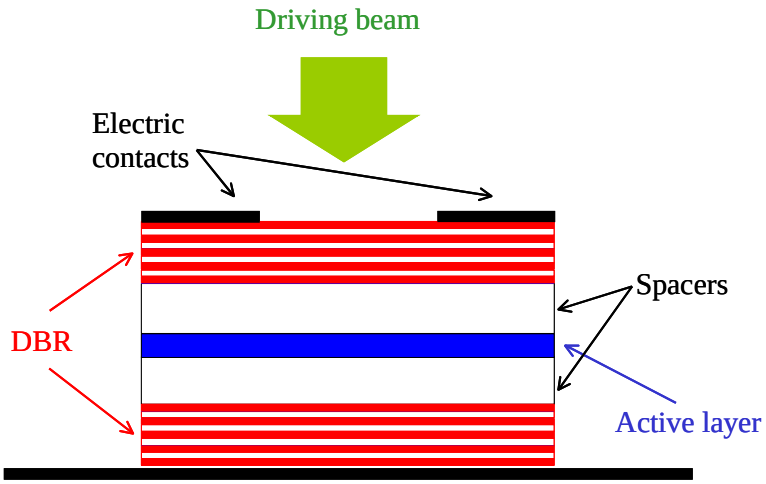

Fig. 1. Scheme of the broad-area vertical-cavity semiconductor microresonator.

terms of excitability of the system. Furthermore, thermal effects can influence not only the global dynamics of the coherent field, but can also introduce local modifications of the refractive index which could result in structure confinement [14].

We report here the occurrence of a thermally induced dynamical instability of the Hopf type, leading to Regenerative Oscillations and to travelling patterns and cavity solitons [15, 16]. These phenomena will be analyzed by performing the numerical integration of the equations describing field, carrier and temperature spatio-temporal dynamics, and adopting the microscopic description for the nonlinear susceptibility. These are five coupled partial differential equations with time constants spanning over 5 or 6 order of magnitude, and so very demanding from the computational time viewpoint. Here we report numerical simulations in two dimensions for the complete model, going beyond the one dimensional picture shown in [15, 16].

In addition, we show movies which illustrate in the best way the dynamical effects induced by the thermal dynamics. The prediction of such dynamical effects has been recently confirmed and extended using a much simpler model for the electronic nonlinearity [17].

2 The model

The device we study is a broad-area vertical-cavity semiconductor microresonator of the Fabry-Perot type (Fig. 1), with Distributed Bragg Reflectors (DBR) as mirrors and driven by an external coherent field. Embedded between the DBR, we consider either a passive layer of bulk GaAs or an active material consisting of few Quantum Wells of GaAs/AlGaAs type. In the latter case an electrical current creates the population inversion in the active material, but the injection level is slightly below the laser threshold.

The dynamics of the system can be described by considering the intracavity electric field, the carrier density in the active material and the temperature of the device.

As for the analysis of the temperature dynamics performed in [16], we just mention that the plasma temperature is adiabatically eliminated and considered equal to the lattice temperature due to the assumption that it has a much faster dynamics than the lattice temperature [18]. Furthermore, the latter is assumed to have a dynamics much

#1519 - $15.00 US
Received August 01, 2002; Revised September 13, 2002

slower with respect to the carrier density dynamics.

The dynamical equations ruling the spatio-temporal behavior of the system variables, derived in the paraxial and slowly varying envelope approximations, mean field limit and single longitudinal mode approximation, can be cast in the following form [16]:

$$\frac{\partial E}{\partial t} = -\kappa \left[(1 + \mathrm{i}\theta(T))E - E_I - \mathrm{i}\Sigma\chi_{nl}(N, T, \omega_0)E - \mathrm{i}\nabla_\perp^2 E \right] , \quad (1)$$

$$\frac{\partial N}{\partial t} = -\gamma \left[N - \mathrm{Im}\left(\chi_{nl}(N, T, \omega_0)\right) |E|^2 - I - d\nabla_\perp^2 N \right] , \quad (2)$$

$$\frac{\partial T}{\partial t} = -\gamma_{th} \left[(T - 1) - D_T \nabla_\perp^2 T \right] + \gamma Z N + \gamma P I^2 , \quad (3)$$

where E is the adimensional slowly varying envelope of the intracavity electric field; N and T are the carrier density normalized to the transparency value N_0 and the temperature normalized to the room temperature T_0, respectively.

The parameters κ, γ and γ_{th} are the decay rates of E, N and T, respectively. We assumed for the ratio between γ_{th} and γ a typical value of 10^{-3}, *i.e.* we consider a temperature dynamics on a microsecond scale, and a carrier dynamics on nanosecond scale. As for the electric field dynamics, it is 2 or 3 order of magnitude faster than carrier dynamics for such a kind of microresonators.

The transverse Laplacian is defined as usual: $\nabla_\perp^2 = \partial^2/\partial x^2 + \partial^2/\partial y^2$; it represents diffraction (in Eq. (1)), and carrier and thermal diffusion (in Eqs. (2) and (3) through the diffusion parameters d and D_T, respectively) in the paraxial approximation. The transverse coordinates x and y are scaled to the diffraction length. ω_0 is the reference frequency; E_I is the adimensional slowly varying envelope of the injected field; I is the adimensional injected current; Σ is the bistability parameter. On the other hand, the coefficients Z and P describe the heating of the device due to carriers and to Joule effect, respectively.

As for the material susceptibility χ_{nl}, we adopt here the microscopic description of the radiation-matter interaction already described in [11]. There, a constant temperature, equal to the room temperature T_0, was assumed. Here, instead, the temperature dependence in the material susceptibility χ_{nl} is taken into account. It mainly consists in a red shift of the band gap ϵ_{gap} of the semiconductor upon an increase of temperature [16].

In order to take into account the thermal shift of the cavity frequency in our model, we have considered a linear dependence on temperature in the cavity detuning θ, this effect being related to the material layers in the regions between the nonlinear medium and the reflectors:

$$\theta = \theta_0 - \alpha(T - 1) , \quad (4)$$

where θ_0 is the cavity detuning at room temperature and α is a parameter related to the variation of the material refractive index with respect to temperature.

For the sake of completeness, we also introduce the band-gap detuning parameter $\Delta = (\epsilon_{gap}(T_0)/\hbar - \omega_0)/\gamma_p$, with γ_p being the polarization decay rate.

For a full description of the system parameters we refer to [16].

3 Numerical results

In this section we show the main results due to the effect of thermal dynamics arising in the transverse plane of the electromagnetic field transmitted by these devices.

The numerical integration of Eqs. (1-3) was performed by using a split-step method with periodic boundary conditions. This method implies the separation of the algebraic and the Laplacian terms in the right-hand side of Eqs. (1-3). In spite of the difficulties

#1519 - $15.00 US Received August 01, 2002; Revised September 13, 2002

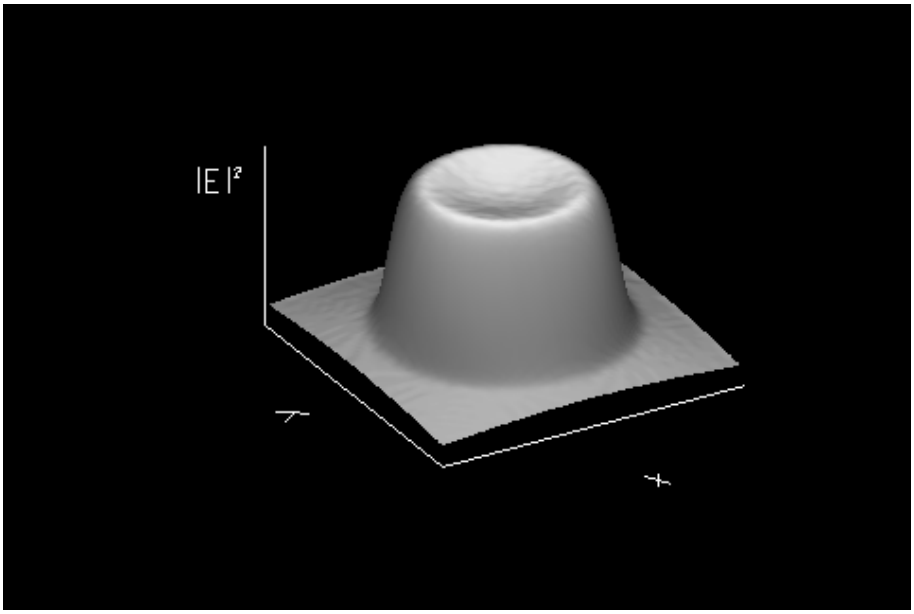

Fig. 2. (File size 1.77 MB) Movie showing the onset of Regenerative Oscillations in the passive configuration with a gaussian input field profile: we report the field intensity transverse cross-section. Integration window is about 140×140 μm wide, while the evolution time is 30 μs. Temporal parameters are: $\kappa^{-1} = 10\,\text{ps}$, $\gamma^{-1} = 10\,\text{ns}$, $\gamma_{th}^{-1} = 20\,\mu\text{s}$. Other parameters are $\Delta = -3$, $\theta_0 = 0$, $\alpha = 5$, $Z \simeq 2.06 \cdot 10^{-3}$, $\Sigma = 80$, $E_I = 27$.

linked to the presence of three very different time scales, spanning over 6 orders of magnitude, the numerical integration was performed in two dimensions. As for the nonlinear susceptibility χ_{nl}, it has been calculated and tabulated in a file as a function of N and T, and then interpolated during the time integration [16].

As a first case we consider the passive configuration with a bulk GaAs as nonlinear material. A linear stability analysis was performed to study the stationary/dynamical instabilities affecting the system. The most common scenario that emerges in the passive case is very similar to the case without thermal effects, that is, the homogeneous steady state is unstable against perturbations modulated in space (Turing instability) and the system is lead to a spatially modulated stationary state. In these cases the Hopf instability domain is entirely inscribed in the Turing domain. As a consequence, when the homogeneous steady state becomes unstable, stationary patterns form spontaneously or, starting from a stable homogeneous steady state, we can excite a stable CS.

Nevertheless, in small regions of the parameter space, close to nascent bistability, the Hopf instability dominates over the spatial Turing instability. When this happens, the Hopf instability is mostly plane-wave, that is, it is characterized by a wavevector $K = 0$. Correspondingly, global regenerative oscillations [12], arise. In Fig. 2 we report a numerical simulation showing the onset of regenerative oscillations for the complete model (1-3) in the case of two transverse dimensions and gaussian input field profile.

Moreover, we found a case where the Hopf instability dominates over the Turing instability and it is characterized by $K \neq 0$. In this case the steady state curve is monostable and no cavity solitons are present. By means of numerical simulations in two transverse dimensions we showed the existence of a travelling pattern in the unstable region. In Fig. 3 we show a movie that demonstrates this result (travelling honeycomb pattern).

Next, we focus our attention on the device with the inverted MQW structure. We

#1519 - $15.00 US Received August 01, 2002; Revised September 13, 2002

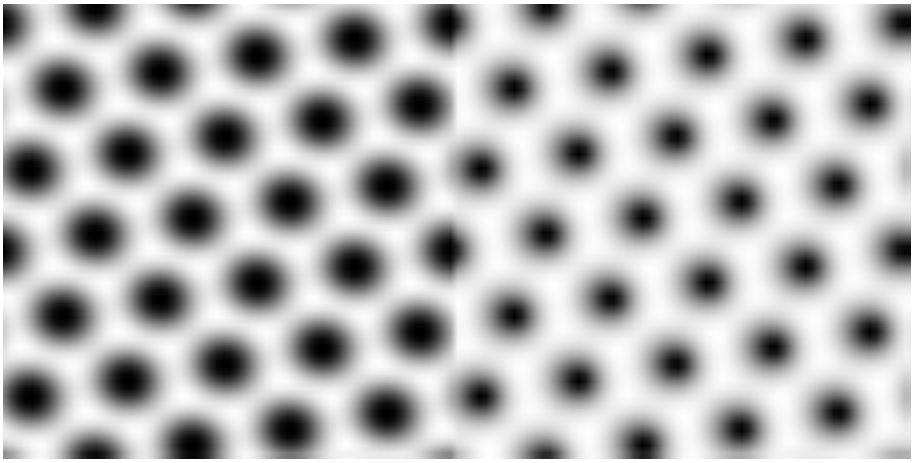

Fig. 3. (File size 1.71 MB) Movie showing the formation of a travelling honeycomb pattern in the transverse cross-section of the field intensity (left) and temperature (right), in the case of the passive configuration: integration window is about 140 $\times$ 140 μm wide, while the evolution time is 24 μs. White corresponds to field intensity and temperature maxima. Temporal parameters are set as in Fig. 2. Other parameters are $\Delta = -1$, $\theta_0 = -6$, $\alpha = 10$, $Z \simeq 2.06 \cdot 10^{-3}$, $\Sigma = 40$, $E_I = 15.5$.

found that carrier and thermal diffusions play an important role in determining what kind of instability will affect the system, because a variation in these parameters can modify strongly the instability boundaries. In particular, for a given choice of the system parameters, we observed the existence of a modulational Hopf instability that dominates the dynamical behavior of the system [16], due to the thermal dynamics. Correspondingly, we showed the existence of a travelling pattern in one/two transverse dimensions.

We studied also the influence of thermal effect on CS. To this aim, we switched on a CS by exploiting the usual superposition of a narrow gaussian pulse on top of the holding beam for a value of the holding beam, where the lower branch of the homogeneous solution is stable. After the CS formation, we observed that it persists in the position where it has been excited for a time on the order of γ_{th}^{-1}, and then it starts drifting. In Fig. 4 we show a movie with the plot of the evolving intensity and temperature profiles in the 1-D case, when a CS is excited in the center of the integration window; this figure allows us to understand what happens. After the excitation of the CS, a minimum appears in the temperature profile, in the spatial location where the CS was created. This is due to the fact that where there is a maximum of the field intensity there are less carriers and then less heating. When the temperature in the minimum reaches a value such that the CS would be no longer stable, it starts moving, following the temperature gradient, towards larger values of temperature, until a dynamical equilibrium among the system variables is reached. This picture was also confirmed by numerical simulations of Eqs. (1) and (2) performed with not evolving temperature profile.

In Fig. 5 we show a movie which confirms that the same behavior is valid also when two transverse dimensions are considered. The excited CS, after a lag of time on the order of γ_{th}^{-1}, starts travelling in the transverse plane.

Furthermore, in Fig. 6, we report the case of two interacting CS. After having been excited, they start moving due to thermal effects in random directions. When they eventually become close enough to feel each other, they interact fusing together into one CS. Finally, after a while, this new CS starts drifting again as in Fig. 5.

#1519 - $15.00 US Received August 01, 2002; Revised September 13, 2002

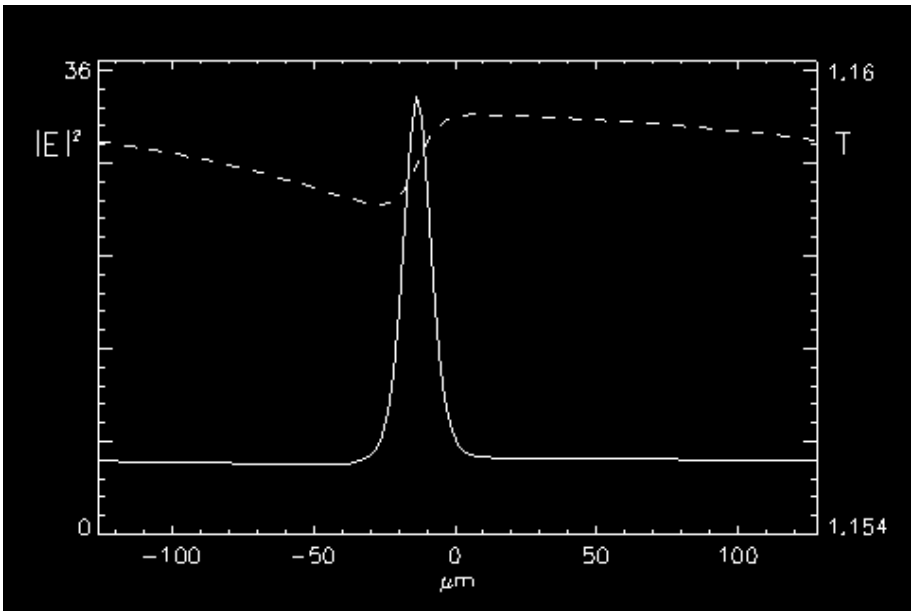

Fig. 4. (File size 1.72 MB) Movie showing the time evolution of the field intensity (solid curve) and temperature (dashed curve) profiles when a CS is excited in the 1-D case, in the active configuration. The evolution time is 6μs. Temporal parameters are: $\kappa^{-1} = 10\,\text{ps}$, $\gamma^{-1} = 1\,\text{ns}$, $\gamma_{th}^{-1} = 1\,\mu\text{s}$. Other parameters are $\Delta = 3$, $\theta_0 = -18.5$, $\alpha = 5$, $\Sigma = 40$, $Z \simeq 1.2 \cdot 10^{-4}$, $P \simeq 8.1 \cdot 10^{-8}$, $I = 1.43$, $E_I = 2.55$.

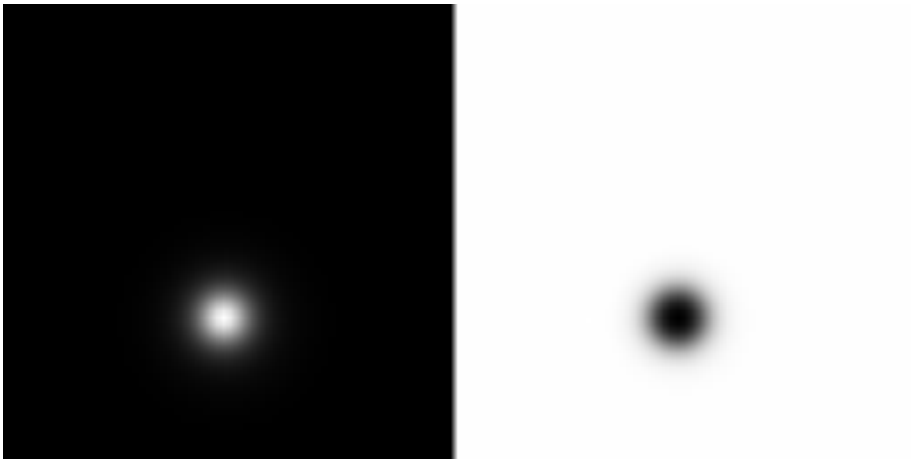

Fig. 5. (File size 273 KB) Movie showing the time evolution of the field intensity (left) and temperature (right) cross-sections after the switching on of a CS, in the active configuration: the integration window is about 125×125 μm wide, while the evolution time is 0.96 μs. White corresponds to field intensity and temperature maxima. Parameters are set as in Fig. 4.

#1519 - $15.00 US Received August 01, 2002; Revised September 13, 2002

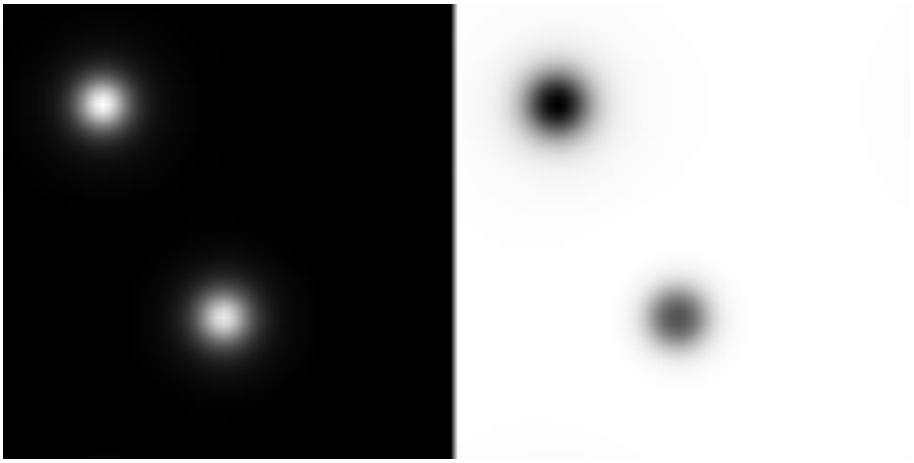

Fig. 6. (File size 397 KB) As in Fig. 5, but with two CS.

4 Conclusions and discussion

In this work we analyzed the interplay between spatio-temporal dynamics and thermal effects in externally-driven semiconductor microresonators with vertical-cavity geometry filled either by bulk GaAs or by an inverted MQW active material, when the full model is analyzed in one and two transverse dimensions.

We analyzed the instabilities affecting the systems, and found both Hopf and Turing instabilities. In the passive (bulk) case, in most regimes, Turing instability dominates over Hopf instability, in such a way that pattern formation is completely unaffected by the presence of thermal effects, and stable cavity solitons can be obtained in wide parametric ranges. When Hopf instability prevails, it is mostly characterized by a zero spatial wavevector, meaning that no patterns can develop. As a matter of fact the Hopf instability in such a case gives rise to Regenerative Oscillations, *i. e.* a regime where the system displays an oscillatory homogeneous output intensity, for a constant homogeneous input intensity. Moreover the numerical simulations performed here led us to concluding that regenerative oscillations appear close to conditions of nascent hysteresis, when an interval of values of the driving field exists where no stationary solution is stable. Finally, a very small parameter range was found, where the Hopf instability was dominating over the Turing instability for $k \neq 0$. In this case the steady state curve is monostable and no cavity solitons are present. In the unstable branch, numerical simulations showed the existence of a travelling honeycomb pattern, showed here by a 2-D movie. This behavior of travelling spatial pattern is just due to the presence of thermal effects.

On the other hand, in the active (MQW) case, the numerical analysis led us to concluding that the system is mostly dominated by a dynamical modulational instability, in such a way that travelling spatial patterns develop. Under the same conditions, cavity solitons are also possible, and after their excitation, they start travelling in one of the two opposite directions that are possible in 1-D geometry, or in a random direction in the 2-D case. In a movie concerning the 1-D case, we showed how the system reaches a spatially modulated dynamical equilibrium state, where the field and temperature profiles reach a stationary shape that travels across the transverse section of the device. Moreover, in the 2-D case we excited two cavity solitons in two different positions: after a while they start to move, then they merge into one cavity soliton. Then the new cavity soliton starts drifting due to thermal effects.

We note that in [17] a narrow parametric domain is identified, where dark cavity

#1519 - $15.00 US Received August 01, 2002; Revised September 13, 2002

solitons are predicted in the passive case. Such dark CS are shown to exhibit a drift motion closely similar to that of bright CS in the active case.

5 Acknowledgments

This work was carried out in the framework of the ESPRIT LTR Project PIANOS *Processing of Information by Arrays of Nonlinear Optical Solitons* and of the PRIN project *Formazione e controllo di solitoni di cavità in microrisonatori a semiconduttore* of the Italian Ministry for University and Research.

#1519 - $15.00 US Received August 01, 2002; Revised September 13, 2002